

General CAV platoon considering the time-varying communication delay: system modeling and stability

Tiancheng Ruan, Hao Wang, Xiaopeng Li, Gengyue Han, Beier Ba, Changyin Dong,

Abstract—Driven by the potential of connected autonomous vehicles (CAVs), recent research has concentrated on their prospective advantages in terms of safety, emissions, and capacity. However, realizing these benefits necessitates ensuring stability, which is the primary objective of CAVs. Although feedback control is widely employed to achieve stability, it cannot be absolutely guaranteed due to the inherent communication delay in CAVs. To tackle this challenge, substantial research has been undertaken to establish stability conditions that account for communication delays. Nevertheless, the majority of this research has implicitly assumed a constant communication delay, representing the maximum delay, which fails to capture the reality of a time-varying delay influenced by the surrounding environment. Consequently, this paper introduces a general supermatrix modeling approach for the CAV platoon considering the time-varying communication delay. Moreover, a novel stability condition, accounting for the time-varying delay in the general CAV platoon, is derived using the Lyapunov-Krasovskii Stability Theorem and Wirtinger-Based Integral Inequality. Extensive numerical analyses in various scenarios are performed to assess the tracking performance and safety conditions of different control parameters and information flow topologies (IFTs). The findings reveal that all CAVs exhibit smooth tracking performance when stability is assured. Enhancing the gain of spacing and velocity errors can improve tracking performance and safety conditions, whereas increasing the gain of acceleration errors cannot. Additionally, leader-based and bi-directional communications facilitate superior tracking and transient performance.

Index Terms—Connected and Automated Vehicles (CAVs); Time-varying communication delay; CAV platoon; Stability analysis; Tracking performance.

I. INTRODUCTION

AUTOMOTIVE engineers have been tirelessly committed to enhancing the safety and comfort of automobile travel since its inception over a century ago. However, traffic problems such as traffic congestion, accidents, and pollutant emissions have become more prominent in recent decades [1, 2, 3]. Traditional traffic engineers have implemented external measures such as traffic management and traffic control to address these issues [4]. However, these measures are becoming increasingly ineffective and are encountering bottlenecks [5]. Research on the static and dynamic characteristics of

T. Ruan, H. Wang, G. Han, B. Ba and C. Dong are with the School of Transportation, Southeast University, Nanjing 211189, P.R. China; Jiangsu Key Laboratory of Urban ITS, Southeast University, Nanjing, 210096, P.R. China; Jiangsu Province Collaborative Innovation Center of Modern Urban Traffic Technologies, Southeast University, Nanjing, 210096, P.R. China(e-mail: ruantiancheng@seu.edu.cn; haowang@seu.edu.cn; gyhan@seu.edu.cn; 980794728@qq.com; dongcy@seu.edu.cn).

Xiaopeng. Li is with Department of Civil & Environmental Engineering, University of Wisconsin-Madison, Madison, 53706, USA(e-mail: xli2485@wisc.edu).

Manuscript received March 2, 2023.(Corresponding author: Hao Wang.)

traffic flow has identified the heterogeneity of human factors as the primary cause of this phenomenon [6, 7, 8, 9].

Automated Vehicles (AVs) have emerged as a promising enabler, benefiting from advancements in technology, and have made significant strides in both the automotive industry and academia in recent years. AVs measure the state error relative to their predecessors through on-board sensing devices, enabling precise tracking [10]. Due to their simplicity and effectiveness, AVs are increasingly regarded as a standard device for modern commercial vehicles, and their market penetration rate (MPR) is growing [11, 12]. Consequently, much research on AVs has revealed their superiority over human-operated vehicles in terms of capacity, safety, and emissions [13, 14, 15].

However, AVs are restricted by limited access to information and, therefore, cannot fully utilize the potential of autonomous driving. Thanks to the advancement of wireless communication technology and Cellular Vehicle-to-Everything (C-V2X), Connected Automated Vehicles (CAVs) have emerged. Equipped with Vehicle-to-Infrastructure (V2I) and Vehicle-to-Vehicle (V2V) communication, CAVs can acquire information more accurately and with less delay, even beyond the sight [16, 17]. Moreover, CAVs have the potential to implement more elaborate platoon control strategies compared to AVs [18, 19], enabling the CAV platoon to leverage further the safety and capacity gains of CAVs [20, 21]. Currently, extensive research has been conducted on CAVs, including the exploration of their capacity gains [22, 23], safety improvement [24, 25, 26], and reduction of pollutant emissions [27, 28].

Despite the advantages mentioned above of CAVs, their stability is the primary goal and prerequisite for utilizing these benefits [29]. Specifically, transient response caused by perturbation fades with time [30]. However, due to unavoidable communication delays, stability cannot be absolutely guaranteed by widely adopted feedback control [31]. Communication delays can cause changes in the timing of a system's response, resulting in phase shifts. When attempting to address this challenge, using feedback control to stabilize a system with time delays may lead to issues. The stability domain may contract, and the likelihood of overcompensation may increase. Overcompensation is a situation in which a system's corrective actions are too forceful, resulting in unwanted oscillations or instability instead of achieving the desired stability. Therefore, abundant research has been conducted to derive stability conditions considering delays [32, 33, 34, 35, 36, 37].

Although numerous methods are utilized in current research, they can be broadly categorized into two main groups: frequency domain-based methods and time domain-based

methods. In early research, stability conditions were mainly derived through frequency domain-based methods [38, 39]. Herman et al. [32] implemented a Laplace transform-based approach for a simple linear time-delay model and derived its characteristic equations. Subsequently, the stability conditions were determined using numerical methods. Zhang and Jarrett [33] expanded this approach by incorporating the product of sensitivity and reaction time in a linear time-delay model, obtaining a more general and analytic stability condition through a characteristic equation-based method. Kamath et al. [36] linearized the optimal velocity model and the classical car-following model to formulate the characteristic equation, taking reaction delay into account, and then applied the Nyquist stability criterion to derive the corresponding stability conditions. In frequency domain-based methods, the communication delay is incorporated into the term $e^{-j\omega\tau}$, where ω is the angular frequency and τ is the communication delay. The delay term implying frequency-dependent phase shift causes a continuous phase change across the entire frequency spectrum, leading to high dimensionality. This high dimensionality poses a challenge for analytically deriving stability conditions in frequency domain-based methods. To address this, linearization techniques such as Fourier's form $e^{ix} = \cos x + i \sin x$ or Euler's formula $f(x) = f(a) + f'(a)(x - a) + \frac{f''(a)}{2!}(x - a)^2 + \dots$ are employed to transform functional differential equations into ordinary differential equations [40]. However, this linearization introduces approximations, which may lead to reduced precision and inaccuracies in stability conditions derived using frequency domain-based methods.

Time domain-based methods, specifically the Second Lyapunov-based methods, have shown superiority in stability analysis for systems with delays. These methods utilize state-space representation to incorporate communication delays into time-delayed states and solve them using advanced mathematical tools, such as the Linear Matrix Inequality approach. For example, Li et al. [34, 35] utilized the full velocity difference car-following model and the Second Lyapunov method to derive a stability condition. They also conducted simulations to assess the dynamic performance under various parameter settings. Gao et al. [41] developed a third-order state-space equation to describe CAV platoon state dynamics with delays and derived the corresponding stability conditions using a delay-dependent Lyapunov function. This function includes a linear quadratic term of states. Guo et al. introduced a double flow controlled two-lane traffic system that utilizes vehicle-to-infrastructure communication. They analyzed the system using the Second Lyapunov method and provided a sufficient stability condition in linear matrix inequality[42]. Moreover, Sun et al. [37] presented a comprehensive review of these methods and validated the consistency and applicability of certain stability conditions through numerical simulations. However, considering time delays in stability analysis requires taking into account not only the current state of the system but also its past states. The dependency on past states introduces an infinite-dimensional aspect to the problem, which requires the extension of the Second Lyapunov method to the functional space to solve stability conditions considering delays. The ex-

tension process adds additional constraints that the Lyapunov functional must hold along all system trajectories, resulting in conservatism in the obtained stability conditions [43, 44, 45]. Consequently, a stability analysis method capable of handling delays without introducing additional constraints must be developed to achieve more accurate stability conditions.

Another limitation of previous research is that they assume communication delay is a constant delay representing the maximum communication delay [46, 47]. However, in reality, the communication delay is time-varying, depending on variations in the surrounding environment [48, 49]. When facing time-varying delay, the two aforementioned methods encounter even more challenges. For frequency domain-based methods, since time-varying delay is not a single parameter, it must be represented as a function of frequency, which can lead to more complex and difficult-to-analyze mathematical expressions. Additionally, similar to dealing with constant delays, approximations still need to be introduced to avoid transforming the stability analysis problem into theoretically intractable functional differential equations. Moreover, the dynamics of the time-varying delay are difficult to capture by frequency domain representation, which necessitates more approximations and assumptions, such as time-varying delay being periodic [50] or linearizing the system with respect to the time-varying delay [51], which can introduce inaccuracies or limitations in the analysis. As for Second Lyapunov-based methods, time-varying delay must be represented as a function of time, making the mathematical expressions more complex and difficult to analyze. To address this complexity, time-scale separation is one solution, which separates the dynamics of the time-varying delay into fast and slow time scales and treats it as a piecewise constant delay [52]. Another solution is to use approximate models to approximate the transfer function of the time-varying delay, substitute it into the system transfer function, and apply the Second Lyapunov method, such as the Padé approximation $D(s) = (b_0 + b_1 s + \dots + b_m s^m)/(1 + a_1 s + \dots + a_n s^n)$, where $D(s)$ is the transfer function of the time-varying delay, s is the Laplace variable, m and n are integers representing the order of the numerator and denominator, and b_0 to b_m and a_1 to a_n are coefficients that can be determined by fitting the Padé approximation to the time-varying delay [53]. However, these solutions can add complexity to the analysis and may introduce inaccuracies. Additionally, the stability conditions obtained by using frequency domain-based methods and Second Lyapunov-based methods to consider time-varying delay are mostly delay-range-dependent and independent of the delay rate. Consequently, a stability analysis method capable of handling time-varying delay must be developed to achieve more accurate and delay-rate-dependent stability conditions.

Consequently, this paper presents a general supermatrix modeling approach for the CAV platoon, considering the time-varying communication delay. Furthermore, the paper introduces a new stability condition for the general CAV platoon that considers time-varying delay by using the Lyapunov-Krasovskii Stability Theorem. This theorem is more realistic as it only requires the Lyapunov Krasovskii Functional mapping in the Banach space holds along the system trajectory, which is more practical than the strict requirement of the Second

Lyapunov method to hold along all system trajectories. Unlike traditional methods that approximate time-varying delays, the dynamics of time-varying delays can be captured by constructing quadratic function integrals that include time-varying functions. In addition, by properly constructing a Lyapunov-Krasovskii Functional, delay-dependent and rate-dependent stability conditions can be derived. Furthermore, the Wirtinger-Based Integral Inequality is utilized in place of the Jensen inequality to establish lower bounds of quadratic function integrals, thereby obtaining more accurate stability conditions. Moreover, comprehensive numerical analyses in various scenarios are conducted to thoroughly evaluate the tracking performance and safety conditions of different control parameters, providing guidance for their selection. In summary, the primary contributions of this paper encompass three aspects:

- 1) A novel stability condition is derived for the CAV platoon, considering the time-varying delay within the general representation, based on the Lyapunov-Krasovskii Stability Theorem.
- 2) The Wirtinger-Based Integral Inequality is utilized in place of the Jensen inequality to obtain a more accurate stability condition.
- 3) Comprehensive numerical analyses in various scenarios are conducted to thoroughly evaluate the tracking performance and safety conditions of different control parameters, offering guidance for their selection.

The structure of the paper is as follows: Section II presents the proposed supermatrix modeling approach for the CAV platoon, considering time-varying communication delay and a corresponding general representation. Section III encompasses the stability analyses and derivation of stability conditions. Section IV evaluates the tracking performance and safety conditions of various control parameters through performance evaluation analysis. Finally, Section V provides a summary of the paper.

Notations throughout the paper:

\mathbb{R}^n denotes the n-dimensional Euclidean space with Euclidian norm $|\cdot|$.

$\mathbb{R}^{m \times n}$ deontes the set of all $m \times n$ real matrices.

\mathbb{S}_n means the set of symmetric matrices of $\mathbb{R}^{n \times n}$.

\mathbb{S}_n^+ denotes the set of symmetric positive definite matrices.

A^T stands for the transpose of a vector or a matrix A .

The symmetric matrix $\begin{bmatrix} A & B \\ * & C \end{bmatrix}$ denotes $\begin{bmatrix} A & B \\ B^T & C \end{bmatrix}$.

$H_e(K)$ represents $K+K^T$ for any square matrix $K \in \mathbb{R}^{n \times n}$.

I_n defines the identity matrix of $n \times n$.

$0_{m,n}$ denotes the zero matrix of $m \times n$ dimension.

For any matrix $A \in \mathbb{R}^{n \times n}$, $A > 0$ denotes that A is symmetric and positive definite.

The Banach space $C([-h, 0], \mathbb{R}^n)$ refers to the set of continuous functions from the interval $[-h, 0] \subset \mathbb{R}$ to \mathbb{R}^n that are square integrable.

For any function $f \in C$, the uniform norm $|f|_h$ refers to $\sup_{\theta \in [-h, 0]} |f(\theta)|$.

$\text{diag}\{a_1, a_2, \dots, a_n\}$ stands for the diagonal matrix

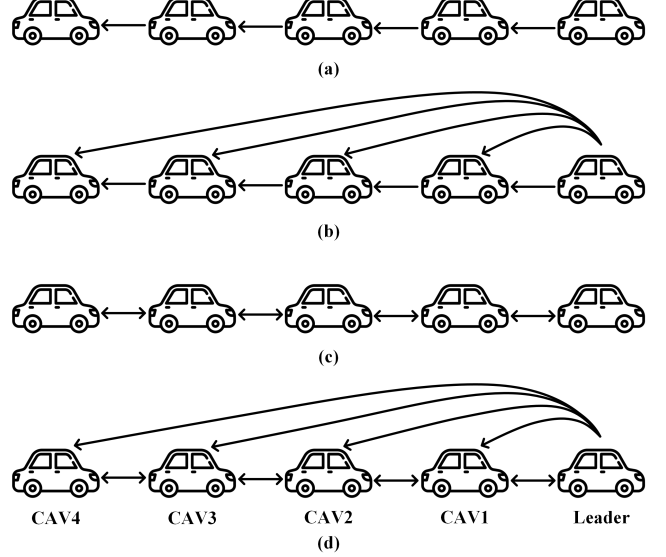


Fig. 1: The schematic of the CAV platoon with typical IFTs, where arrows indicate the direction of information transmission, with unidirectional arrows representing one-way communication and bidirectional arrows representing two-way communication: (a) Predecessor-Follower (PF); (b) Predecessor-Leader-Follower (PLF); (c) Bi-Directional (BD); and (d) Bi-Directional-Leader (BDL).

$\begin{bmatrix} a_1 & 0 & 0 \\ 0 & \ddots & 0 \\ 0 & 0 & a_n \end{bmatrix}$ whose diagonal elements from the top left corner are a_1, a_2, \dots, a_n .

Let $A \in \mathbb{R}^{m \times n}$ and $B \in \mathbb{R}^{p \times q}$. The Kronecker product of A and B is denoted as $A \otimes B$ and defined as follows:

$$A \otimes B = \begin{bmatrix} a_{11}B & \cdots & a_{1n}B \\ \vdots & \ddots & \vdots \\ a_{m1}B & \cdots & a_{mn}B \end{bmatrix} \in \mathbb{R}^{mp \times nq}.$$

Let $C \in \mathbb{R}^{m \times n}$ and $D \in \mathbb{R}^{n \times n}$. The Hadamard product of C and D is denotes as $C \circ D$ and defined as follows:

$$C \circ D = \begin{bmatrix} c_{11}d_{11} & \cdots & c_{1n}d_{1n} \\ \vdots & \ddots & \vdots \\ c_{m1}d_{m1} & \cdots & c_{mn}d_{mn} \end{bmatrix} \in \mathbb{R}^{m \times n}.$$

II. SYSTEM MODELING

In this scenario, a platoon of n CAVs is traveling along a single lane, and the intra-vehicle communication is carried out in accordance with the IFT protocol. Fig.1 illustrates the schematic of the CAV platoon with four typical IFTs, where arrows indicate the direction of information transmission, with unidirectional arrows representing one-way communication and bidirectional arrows representing two-way communication: (a) Predecessor-Follower (PF), (b) Predecessor-Leader-Follower (PLF), (c) Bi-Directional (BD), and (d) Bi-Directional-Leader (BDL). By treating the vehicles in the platoon as nodes and the intervehicle communication as edges, a

weighted directed graph $\mathcal{G} = \{\mathcal{V}, \mathcal{E}, \mathcal{A}\}$ models the information flow topology (IFT) among the platoon. Within the digraph \mathcal{G} , $\mathcal{V} = \{1, 2, \dots, n\}$ denotes the nodes set and $\mathcal{E} \subseteq \mathcal{V} \times \mathcal{V}$ represents edges set. Besides, \mathcal{A} is the weighted adjacent matrix with nonnegative elements defined as $\mathcal{A} = [a_{ij}]_{n \times n}$ with $a_{ii} = 0$ which denotes that the self-edge (i, i) is forbidden except as noted. Moreover, the edge (i, j) in \mathcal{E} signifies the communication between vehicle i and vehicle j associated with weighted a_{ij} . Defining the degree matrix of \mathcal{G} as $\mathcal{D} = \text{diag}\{d_1, d_2, \dots, d_n\}$, with $d_i = \sum_{j \in \mathcal{V}} a_{ij}$. Within the time duration,

the longitudinal position, speed, acceleration, and jerk of vehicle $i \in \mathcal{V}$ at time t are denoted as $p_i(t)$, $v_i(t) = \dot{p}_i(t)$, $a_i(t) = \ddot{p}_i(t)$, and $\dot{a}_i(t) = \dddot{p}_i(t) \in \mathbb{R}$, respectively. Via intra-vehicle communication (e.g., C-V2X according to the meeting report from the Federal Communications Commission [54]), all vehicles within the platoon exchange state information, such as absolute position, velocity, and acceleration, with their neighboring vehicles in accordance with the IFT protocol. It is assumed that each CAV is equipped with the following components: (i) an on-board radar for detecting potential collisions by measuring the gap distance between consecutive vehicles, (ii) a GPS sensor for obtaining the longitudinal position, (iii) a wireless on-board unit that enables communication of relevant information with proximal vehicles via C-V2X communication [55], (iv) an upper-level controller that calculates the desired longitudinal acceleration based on the obtained parameters, and (v) a lower-level controller that determines the throttle and brake actuator inputs to follow the desired acceleration. This assumption is justifiable, as the sensing, communication, and actuation units listed above are standard features in modern CAVs and hence do not require any additional modifications to the existing vehicle configuration. It should be noted that the information obtained by the on-board radar regarding the surrounding environment only serves as a validation check in the event of communication unavailability or failure. This is because communication-based exchange of information is more efficient and provides more accurate data, rendering the use of radar as a supplementary measure rather than a primary source of information.

A. Vehicle longitudinal dynamic Modeling

The longitudinal dynamics of vehicle i can be mathematically formulated by accounting for various resistance forces influenced by the engine, throttle and brake actuators, drive train, transmission, and torque converter. The resulting model, based on the fundamental principles of Newton's second law, can be represented by the following equation:

$$m_i a_i(t) = f_i^e(t) - f_i^g(t) - f_i^w(t) - f_i^r(t), \quad (1)$$

where m_i stands for the unknown mass of vehicle i ; $f_i^e(t)$ is the desired engine force acting on the vehicle i ; $f_i^g(t)$, $f_i^w(t)$, and $f_i^r(t)$ denote the gravity component parallel to the road surface, air resistance force, and rolling resistance force, respectively.

The nonlinearity of the system (1) makes it challenging to controller design challenging. Therefore, a feedback control

input in Appendix A is employed to convert it into a linear form [56]:

$$\tau_i \dot{a}_i(t) + a_i(t) = u_i(t), \quad (2)$$

where $u_i(t)$ denotes the control input of the lower-level controller, which can be interpreted as the desired acceleration of vehicle i , τ_i denotes the time constant that represents the delay caused by the engine actuator.

Reformulate Equation (2), the state space equation can be represented as:

$$\dot{x}_i(t) = Ax_i(t) + Bu_i(t), \quad (3)$$

$$\text{with } A = \begin{bmatrix} 0 & 1 & 0 \\ 0 & 0 & 1 \\ 0 & 0 & -\frac{1}{\tau_i} \end{bmatrix} \text{ and } B = \begin{bmatrix} 0 \\ 0 \\ \frac{1}{\tau_i} \end{bmatrix},$$

where $x_i(t) = \begin{bmatrix} p_i(t) & v_i(t) & a_i(t) \end{bmatrix}^T \in \mathbb{R}^3$ denotes the state vector of vehicle i .

Subject to limited communication, the inputs for vehicle i are controlled by an appropriate decentralized coupling protocol of communication information:

$$u_i = u_i \underbrace{(x_1(t-h(t)), \dots, x_i(t), \dots, x_n(t-h(t)))}_n, \quad (4)$$

where $h(t)$ represents the time-varying communication delay within the transmission range which is assumed to be influenced by the surrounding environment [57, 58, 59, 60, 61]. And it satisfies the following constraints:

$$h(t) \in [h_m, h_M], \quad \dot{h}(t) \in [d_m, d_M], \quad \forall t \geq 0, \quad (5)$$

where $0 \leq h_m \leq h_M$ and $d_m \leq d_M \leq 1$.

Assuming that CAVs adopt the Constant Time Headway (CTH) policy, where CAVs maintain a desired time headway from the reference vehicle, we can formulate the cooperative tracking problem of vehicle i as follows:

$$\begin{cases} \lim_{t \rightarrow \infty} \left\| \sum_{j=1}^n |p_i(t) - p_j(t-h(t)) + h_{ij}v_i(t)| \right\| = 0, \\ \lim_{t \rightarrow \infty} \left\| \sum_{j=1}^n |v_i(t) - v_j(t-h(t))| \right\| = 0, \quad , \forall i = 1, \dots, N. \\ \lim_{t \rightarrow \infty} \left\| \sum_{j=1}^n |a_i(t) - a_j(t-h(t))| \right\| = 0. \end{cases} \quad (6)$$

where $h_{ij} = -h_{ji}$ stands for the constant time headway between vehicle i and vehicle j .

By implementing a suitable distributed control strategy, the consensus objective stated in Equation (6) can be attained. Therefore, the vehicle i updates its dynamics via an onboard computation of the following decentralized coupling protocol:

$$u_i = - \sum_{j=1}^n a_{ij} k_{ij}^T \begin{bmatrix} p_i(t) - p_j(t-h(t)) + h_{ij}v_i(t) \\ v_i(t) - v_j(t-h(t)) \\ a_i(t) - a_j(t-h(t)) \end{bmatrix}, \quad (7)$$

where a_{ij} denotes the weight of edge (i, j) and $a_{ij} = 0$ if there is no edge (i, j) ; $k_{ij} = [\alpha_{ij} \ \beta_{ij} \ \gamma_{ij}]^T \in \mathbb{R}^{3 \times 1}$ presents the feedback control gain vector, with α_{ij} , β_{ij} , and γ_{ij} denoting

the control gain of spacing, speed, and acceleration error, respectively.

B. CAV platoon Modeling

To achieve consensus of systems (3) and (4) under the influence of the coupling protocol (7), it is necessary to reformulate the decentralized coupling protocol (7) as follows:

$$u_i = - \sum_{j=1}^n a_{ij} k_{ij}^T [\psi_{ij} x_i(t) - x_j(t-h(t))], \quad (8)$$

where $\psi_{ij} = \begin{bmatrix} 1 & h_{ij} \\ & 1 \\ & & 1 \end{bmatrix}$ denotes the relationship between the states based on the CTH policy.

Therefore, the dynamics of the error system can be presented as:

$$\begin{cases} \dot{\tilde{p}}_i = \tilde{v}_i, \\ \dot{\tilde{v}}_i = \tilde{a}_i, \\ \dot{\tilde{a}}_i = -\frac{1}{\tau} \tilde{a}_i - \frac{1}{\tau} \sum_{j=1}^n a_{ij} k_{ij}^T (\psi_{ij} x_i(t) - x_j(t-h(t))). \end{cases} \quad (9)$$

From Equation (9), the dynamics of the closed-loop vehicular network can be reformulated using supermatrices, resulting in a more concise representation:

$$\dot{x}_i(t) = Ax_i(t) - B \sum_{j=1}^n a_{ij} k_{ij}^T (\psi_{ij} x_i(t) - x_j(t-h(t))). \quad (10)$$

Theorem 1. *The CAV platoon under CTH policy with time-varying communication delay can be modeled as a linear time-invariant state time-varying delay system:*

$$\begin{cases} \dot{X}(t) = \Psi X(t) + \Psi_d X(t-h(t)), & \forall t \geq 0 \\ X(t) = \phi(t), & \forall t \in [-h, 0] \end{cases} \quad (11)$$

with

$$\left\{ \begin{array}{l} \Psi = A^* - B^* \mathcal{F} E_1 \in \mathbb{R}^{3n \times 3n} \\ \Psi_d = B^* \mathcal{J} E_2 \in \mathbb{R}^{3n \times 3n} \\ A^* = I_n \otimes A \in \mathbb{R}^{3n \times 3n} \\ B^* = I_n \otimes B \in \mathbb{R}^{3n \times n} \\ \mathcal{K} = [k_{ij}^T]_{n \times n} \\ \mathcal{H} = \mathcal{A} \circ \mathcal{K} = [a_{ij} \otimes k_{ij}^T]_{N \times N} \in \mathbb{R}^{n \times 3n} \\ \mathcal{J} = \text{diag} \underbrace{\{\mathcal{D}_1, \mathcal{D}_2, \dots, \mathcal{D}_N\}}_n \in \mathbb{R}^{n \times 3n^2} \\ \mathcal{D}_i = \underbrace{[a_{i1} k_{i1}^T, a_{i2} k_{i2}^T, \dots, a_{in} k_{in}^T]}_n \in \mathbb{R}^{1 \times 3n}, \forall i \in \mathcal{V} \\ \mathcal{F} = \text{diag} \underbrace{\{\mathcal{H}_1, \mathcal{H}_2, \dots, \mathcal{H}_N\}}_n \in \mathbb{R}^{n \times 3n^2} \\ \mathcal{H}_i = \mathcal{D}_i \circ \underbrace{[\psi_{i1}, \psi_{i2}, \dots, \psi_{in}]}_n \in \mathbb{R}^{1 \times 3n}, \forall i \in \mathcal{V} \\ E_1 = \text{diag} \underbrace{\{I_1, I_1, \dots, I_1\}}_n \in \mathbb{R}^{3n^2 \times 3n} \\ E_2 = \left[\underbrace{I_2^T \ \dots \ I_2^T}_n \right]^T \in \mathbb{R}^{3n^2 \times 3n} \\ I_1 = \left[\underbrace{I_3^T \ \dots \ I_3^T}_n \right]^T \in \mathbb{R}^{3n \times 3} \\ I_2 = I_{3n} \in \mathbb{R}^{3n \times 3n} \\ I_3 = I_3 \in \mathbb{R}^{3 \times 3} \end{array} \right. \quad (12)$$

where $X(t) = [x_1^T \ \dots \ x_n^T]^T \in \mathbb{R}^{3n}$ stands for the error state vector of the closed-loop vehicular network; ϕ is the initial conditions; Ψ and Ψ_d are constant matrix according to their definitions.

III. STABILITY ANALYSES

The Lyapunov-Krasovskii Stability Theorem is a commonly used method for analyzing stability in state delay systems. This approach is an extension of the Second Lyapunov method, which is specifically designed for stability analysis [62]. It involves the use of "energy" functionals that are both positive definite and monotonically decreasing along the system trajectories. The statement of the Lyapunov-Krasovskii Theorem is presented below:

Lemma 2. *(Lyapunov-Krasovskii Stability Theorem [63]). Given system (11), suppose that f maps $\mathbb{R} \times (\text{bounded sets in } \mathbb{R}^n \times C)$ into bounded sets in \mathbb{R}^n , and that $u, v, w : \mathbb{R}_+ \rightarrow \mathbb{R}_+$ are continuous nondecreasing functions, where additionally $u(s)$ and $v(s)$ are positive for $s > 0$, and $u(0) = v(0) = 0$. If there exists a functional $V : \mathbb{R} \times \mathbb{R}^n \times C \rightarrow \mathbb{R}$ such that*

$$\begin{cases} u(|\phi(0)|) \leq V(t, \phi) \leq v(|\phi|_h), \\ \dot{V}(t, \phi) \leq -w(|\phi(0)|). \end{cases} \quad (13)$$

Then the trivial solution of the system (11) is uniformly stable. If $w(s) > 0$ for $s > 0$, then it is uniformly asymptotically stable. If, in addition, $\lim_{s \rightarrow \infty} u(s) = +\infty$, then it is globally uniformly asymptotically stable. Such a functional V is called a Lyapunov-Krasovskii functional (LKF).

Moreover, integral inequalities provide significant assistance in the study of lower bounds of quadratic function integrals for the stability analysis of state-delayed systems [64, 65, 66]. Among them, Wirtinger Integral inequalities are considered to be effective and less conservative [67, 68]. Wirtinger Integral inequalities are a series of integral inequalities that employ the integral of a function to estimate the integral of its derivative function. The Wirtinger Integral inequality is stated as follows:

Lemma 3. (*Wirtinger Integral Inequality [69]*). *Given a positive definite $n \times n$ matrix R , the following inequality holds for any $z \in C([-h, 0], \mathbb{R}^n)$ that satisfies $z(-h) = z(0) = 0$:*

$$\int_{-h}^0 \dot{z}^T(u) R \dot{z}(u) du \geq \frac{\pi^2}{h^2} \int_{-h}^0 z^T(u) R z(u) du. \quad (14)$$

Although the Jensen inequality [62] is commonly employed in research to establish lower bounds of quadratic function integrals, its inherent conservatism can lead to less precise results. To obtain more accurate lower bounds, the Wirtinger Integral Inequality can be utilized, as highlighted in Remark 6.

Additionally, we present another useful lemma that is motivated by the concept of reciprocally convex combination:

Lemma 4. ([70]) *Let n and m be positive integers, $\alpha \in (0, 1)$ be a scalar, $R > 0$ be a given $n \times n$ matrix, and W_1 and W_2 be two $n \times m$ matrices in $\mathbb{R}^{n \times m}$. The function $\Theta(\alpha, R)$ is defined for all vectors ξ in \mathbb{R}^m as follows:*

$$\Theta(\alpha, R) = \frac{1}{\alpha} \xi^T W_1^T R W_1 \xi + \frac{1}{1-\alpha} \xi^T W_2^T R W_2 \xi. \quad (15)$$

Then, if there exists a matrix X in $\mathbb{R}^{n \times n}$ such that $\begin{bmatrix} R & X \\ * & R \end{bmatrix} > 0$, then the following inequality holds:

$$\min_{\alpha \in (0, 1)} \Theta(\alpha, R) \geq \begin{bmatrix} W_1 \xi \\ W_2 \xi \end{bmatrix}^T \begin{bmatrix} R & X \\ * & R \end{bmatrix} \begin{bmatrix} W_1 \xi \\ W_2 \xi \end{bmatrix}. \quad (16)$$

Lemma 2 aims to establish a positive definite functional whose time derivative is negative definite along the trajectories of the system (11). This forms the core idea behind the lemma. In the context of the stability analysis of such systems using LKF, several types of functionals have been provided in the literature. Among them, an integral quadratic term is one of the most relevant components of LKF [71]:

$$V(X_t) = \int_{0-h}^0 \int_{\theta}^0 \dot{X}_t^T(s) R \dot{X}_t(s) ds d\theta, \quad (17)$$

where $\dot{X}_t(s) = \dot{X}(t+s)$ denotes the state of the state delay system, $R > 0$ and $h > 0$.

The positivity of LKF (17) is ensured by $R > 0$. Then another that needs to be clarified is the negation of its derivative. Differentiating this term with respect to the time t , we get:

$$\dot{V}(X_t) = h \dot{X}^T(t) R \dot{X}(t) - \int_{-h}^0 \dot{X}^T(s) R \dot{X}(s) ds. \quad (18)$$

To transform Equation (18) into a suitable LMI framework, an over-approximation process of the integral terms is required as they cannot be readily converted using the quadratic formulation discussed previously. Consequently, the current task

is to derive a new lower bound of integral quadratic terms in the following format:

$$F(\omega) = \int_{-h}^0 \omega^T(s) R \omega(s) ds, \quad (19)$$

where ω is a continuous function from $[a, b] \rightarrow \mathbb{R}^n$ and consequently integrable.

Corollary 5. *Given a positive definite matrix R , the following inequality holds for all continuous functions $\omega : [a, b] \rightarrow \mathbb{R}^n$:*

$$F(\omega) \geq \frac{1}{h} \left(\int_{-h}^0 \omega(u) du \right)^T R \left(\int_{-h}^0 \omega(u) du \right) + \frac{3}{h} \Omega^T R \Omega, \quad (20)$$

$$\text{where } \Omega = \int_{-h}^0 \omega(s) ds - \frac{2}{h} \int_{-h}^0 \int_{-h}^s \omega(r) dr ds.$$

Proof: We first construct the function z for all $u \in [a, b]$ as:

$$z(u) = \int_{-h}^u \omega(s) ds - \frac{u+h}{h} \int_{-h}^0 \omega(s) ds - \frac{(-u)(u+h)}{h^2} \Theta, \quad (21)$$

where Θ is a constant vector of \mathbb{R}^n to be defined. Moreover, the function $z(u)$ (21) satisfies the constraints of Lemma 3, that is $z(0) = z(-h) = 0$ according to its definition.

Then, calculating the left-hand-side of the inequality mentioned in Lemma 3 yields:

$$\begin{aligned} \int_{-h}^0 \dot{z}^T(u) R \dot{z}(u) du &= 2 \int_{-h}^0 \left(\frac{(-h-2u)}{h^2} \right) du \Theta^T R \left(\int_{-h}^0 \omega(u) du \right) \\ &+ \int_{-h}^0 \left(\frac{(h+2u)}{h^2} \right)^2 du \Theta^T R \Theta - 2 \Theta^T R \int_{-h}^0 \left(\frac{(-h-2u)}{h^2} \right) \omega(u) du \\ &+ \int_{-h}^0 \omega^T(u) R \omega(u) du - \frac{1}{h} \left(\int_{-h}^0 \omega(u) du \right)^T R \left(\int_{-h}^0 \omega(u) du \right). \end{aligned} \quad (22)$$

Substituting $\int_{-h}^0 -h-2u du = 0$ and applying integration by parts, Equation (22) can be simplified as follows:

$$\begin{aligned} \int_{-h}^0 \dot{z}^T(u) R \dot{z}(u) du &= \int_{-h}^0 \omega^T(u) R \omega(u) du \\ &- \frac{1}{h} \left(\int_{-h}^0 \omega(u) du \right)^T R \left(\int_{-h}^0 \omega(u) du \right) \\ &- \frac{3}{(b-a)} \Omega^T R \Omega + \frac{1}{3(b-a)} (\Theta + 3\Omega)^T R (\Theta + 3\Omega). \end{aligned} \quad (23)$$

Substituting $\int_{-h}^0 z(u) du = -\frac{h}{6}(\Theta + 3\Omega)$ and applying Lemma 3, it yields:

$$\begin{aligned} F(\omega) &\geq \frac{1}{h} \left(\int_{-h}^0 \omega(u) du \right)^T R \left(\int_{-h}^0 \omega(u) du \right) + h \Omega^T R \Omega \\ &+ \frac{\pi^2 - 12}{36h} (\Theta + 3\Omega)^T R (\Theta + 3\Omega). \end{aligned} \quad (24)$$

Given that $\frac{\pi^2 - 12}{36h} > 0$, the third term on the right-hand side of the inequality (24) is positive definite, regardless of the selection of Θ . Moreover, the inequality is equivalent to equality if and only if $\Theta = -3\Omega$. Furthermore, the definite positiveness of $F(\omega)$ is guaranteed by $R > 0$.

This concludes the proof. ■

Remark 6. Note that the first term to the right of Inequality (20) is Jensen inequality [62]. Since the second term is definite positive, the lower bound of the integral is evidently higher than the result obtained through Jensen inequality. Therefore, with Wirtinger-Based Integral Inequality, more accurate stability conditions can be obtained.

According to Inequality (18), another lower bound needed to be determined is the case of $F(\dot{\omega})$. Therefore, Corollary 5 is rewritten as follows:

Corollary 7. Given a positive definite matrix R , all continuously differentiable functions $\omega : [a, b] \rightarrow \mathbb{R}^n$ satisfy the subsequent inequality:

$$F(\dot{\omega}) \geq \frac{1}{h}(\omega(0) - \omega(-h))^T R (\omega(0) - \omega(-h)) + \frac{3}{h} \tilde{\Omega}^T R \tilde{\Omega}, \quad (25)$$

where $\tilde{\Omega} = \omega(0) + \omega(-h) - \frac{2}{h} \int_a^b \omega(u) du$.

The subsequent stability theorem is presented below:

Theorem 8. Assuming the existence of $P \in \mathbb{S}_{3n}^+$, three matrices $S, R, Q \in \mathbb{S}^{n+}$, and $X \in \mathbb{S}^{2n}$, the ensuing LMIs hold for $h = h_m, h_M$ and $\dot{h} = d_m, d_M$.

$$\Phi_1(h, \dot{h}) = \Phi_0(h, \dot{h}) - \frac{1}{h_M} \Gamma^T \Phi_2 \Gamma < 0, \quad (26)$$

$$\Phi_2 = \begin{bmatrix} \tilde{R} & X \\ * & \tilde{R} \end{bmatrix} > 0, \quad (27)$$

where

$$\Phi_0(h, \dot{h}) = \text{He}\left(G_1^T(h)PG_0(\dot{h})\right) + \hat{S} + \hat{Q}(\dot{h}) + h_M G_0^T(\dot{h})\hat{R}G_0(\dot{h});$$

$$\Gamma = \begin{bmatrix} K_1^T & K_2^T \end{bmatrix}^T;$$

$$K_1 = \begin{bmatrix} I & -I & 0 & 0 & 0 \\ I & I & 0 & -2I & 0 \end{bmatrix};$$

$$K_2 = \begin{bmatrix} 0 & I & -I & 0 & 0 \\ 0 & I & I & 0 & -2I \end{bmatrix};$$

$$\hat{Q}(\dot{h}) = \text{diag}(Q, -(1-\dot{h})Q, 0_{3n});$$

$$\hat{S} = \text{diag}(S, 0, -S, 0_{2n});$$

$$\hat{R} = \text{diag}(R, 0_{3n});$$

$$\tilde{R} = \text{diag}(R, 3R);$$

$$G_0(\dot{h}) = \begin{bmatrix} \Psi & \Psi_d & 0 & 0 & 0 \\ I & -(1-\dot{h})I & 0 & 0 & 0 \\ 0 & (1-\dot{h})I & -I & 0 & 0 \end{bmatrix};$$

$$G_1(h) = \begin{bmatrix} I & 0 & 0 & 0 & 0 \\ 0 & 0 & 0 & hI & 0 \\ 0 & 0 & 0 & 0 & (h_M - h)I \end{bmatrix}.$$

Then the system (11) is asymptotically stable for all delay function h satisfying (5).

Proof: We first construct the LKF as:

$$V(h, x_t, \dot{x}_t) = \tilde{x}^T(t)P\tilde{x}(t) + \int_{-h(t)}^0 x^T(s)Qx(s)ds + \int_{-h_M}^0 x^T(s)Sx(s)ds + \int_{-h_M}^0 \int_\theta^0 \dot{x}^T(s)R\dot{x}(s)ds d\theta, \quad (28)$$

where $\tilde{x}(t) = \begin{bmatrix} x^T(t), & \int_{-h(t)}^0 x^T(s)ds, & \int_{-h_M}^{-h(t)} x^T(s)ds \end{bmatrix}^T$.

The positivity of LKF (28) is guaranteed by $P > 0$, $Q > 0$, $S > 0$, and $R > 0$. Consequently, the negation of its derivative

needs to be elucidated. Upon differentiating the functional (18) along the trajectories of (11), we obtain:

$$\dot{V}(h, x_t, \dot{x}_t) = \zeta_1^T(t)\Phi_0(h, \dot{h})\zeta_1(t) - \int_{-h_M}^0 \dot{x}^T(s)R\dot{x}(s)ds, \quad (29)$$

$$\text{where } \zeta_1(t) = \begin{bmatrix} x(t) \\ x(t-h(t)) \\ x(t-h_M) \\ \frac{1}{h(t)} \int_{-h(t)}^0 x(s)ds \\ \frac{1}{h_M-h(t)} \int_{-h_M}^{-h(t)} x(s)ds \end{bmatrix}.$$

Notice the Equation (29) can be obtained by substituting $\tilde{x}(t) = G_1(h)\zeta_1(t)$ and $\dot{\tilde{x}}(t) = G_0(\dot{h})\zeta_1(t)$ into the partial differential of Equation (28).

Then split the integral interval of Equation (29) into two parts: $[-h_M, -h(t)]$ and $[-h_M, 0]$, and apply Corollary 7 respectively to get:

$$-\int_{t-h_M}^t \dot{x}^T(s)R\dot{x}(s)ds \leq -\zeta_1^T(t) \left(\frac{1}{h(t)} K_1^T \tilde{R} K_1 + \frac{1}{h_M - h(t)} K_2^T \tilde{R} K_2 \right) \zeta_1(t). \quad (30)$$

Given the constraint of Lemma 4, assuming the existence of X such that $\Phi_2 > 0$, we can conclude that the ensuing inequality holds true:

$$-\int_{t-h_M}^t \dot{x}^T(s)R\dot{x}(s)ds \leq -\frac{1}{h_M} \zeta_1^T(t) \Gamma^T \Phi_2 \Gamma \zeta_1(t), \quad (31)$$

Substituting Inequality (31) into Equation (29), it yields:

$$\begin{aligned} \dot{V}(h, x_t, \dot{x}_t) &\leq \zeta_1^T(t)\Phi_0(h, \dot{h})\zeta_1(t) - \frac{1}{h_M} \zeta_1^T(t) \Gamma^T \Phi_2 \Gamma \zeta_1(t) \\ &= \zeta_1^T(t) \left(\Phi_0(h, \dot{h}) - \frac{1}{h_M} \Gamma^T \Phi_2 \Gamma \right) \zeta_1(t) \\ &= \zeta_1^T(t) \Phi_1(h, \dot{h}) \zeta_1(t). \end{aligned} \quad (32)$$

Equation (32) ensures the negative definiteness of $\dot{V}(h, x_t, \dot{x}_t)$ by imposing the constraint $\Phi_1(h, \dot{h}) < 0$. It is important to note that the matrix $\Phi_1(h, \dot{h})$ is affine and therefore convex with respect to $h(t)$ and $\dot{h}(t)$. Consequently, to guarantee $\Phi_1(h, \dot{h}) < 0$, it is necessary and sufficient to confine it to the vertices of the intervals $[0, h_M] \times [d_m, d_M]$.

To sum up, the negative definiteness of $\dot{V}(h, x_t, \dot{x}_t)$ is ensured if a matrix X exists such that $\Phi_2 > 0$ and $\Phi_1(h, \dot{h}) < 0$ holds for all $(h, \dot{h}) \in [0, h_M] \times [d_m, d_M]$.

This completes the proof. ■

Remark 9. The key idea of the Lyapunov-Krasovskii Stability Theorem is that it is not necessary to establish the negative definiteness of $V(t, X(t))$ along all system trajectories. Rather, it is sufficient to ensure its negative definiteness for solutions that tend to move away from the vicinity of $V(t, X(t)) \leq c$ of the equilibrium. Appendix B offers an in-depth theoretical analysis of this concept.

Remark 10. The code to construct the LMIs in Theorem 8 is available on GitHub for future research purposes. The associated URL can be found in Appendix C for additional reference.

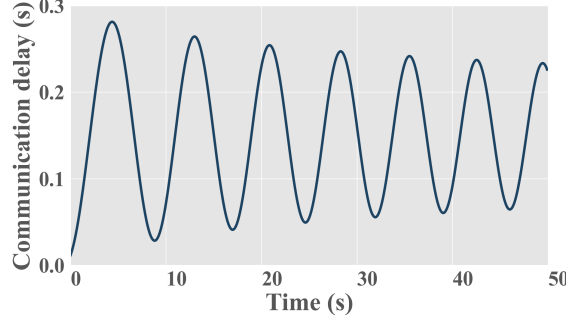


Fig. 2: The curve of time-varying communication delay.

IV. NUMERICAL ANALYSES

In this section, a thorough examination of numerical simulations and analyses is conducted to highlight the primary outcomes. The investigation focuses on the tracking performance and safety conditions of a CAV platoon employing the PLF, with various feedback control gains. Moreover, the tracking performances of the CAV platoon using the remaining three IFTs are also explored.

A. Numerical Setup

For a thorough performance evaluation, a CAV platoon consisting of 5 interconnected CAVs utilizing the PLF, as depicted in Fig.1 (b), is considered. The Leader CAV follows a specified speed profile, while the other CAVs operate under the control strategy. It should be noted that each CAV in the platoon communicates solely with its neighbors in the PLF. Furthermore, control parameters must be set in accordance with the specific control strategy employed. For additional analysis, parameters for both network and traffic simulations are established in Table I, maintaining simplicity without sacrificing generality. It is important to highlight that the weights of the weighted adjacency matrix are set to $a_{ij} = \frac{1}{d_i}, \forall (i, j) \in \mathcal{E}$, indicating that the information from each neighbor has an equal impact on the control decision. Regarding the time-varying delay, the time-varying equation is provided below in the form of the Bessel function of the first kind [72, 73, 74]. The time-varying curve, shown in Fig.2, satisfies the constraint in Equation (5):

$$J_{40}(t) = \sum_{k=0}^{\infty} \frac{(-1)^k}{k!(k+40)!} \left(\frac{t+30}{2} \right)^{2k+40}, \quad t \geq 0. \quad (33)$$

Furthermore, to assess the tracking performance of the CAV platoon under the PLF with varying feedback control gains, two representative leader maneuvers are adopted:

- 1) **Trapezoidal signal:** The leader suddenly decelerates to $14.6 m/s$ at a rate of $-0.15 m/s^2$ and maintains this velocity for $36s$. Subsequently, the leader accelerates back to $20m/s$ at $0.3m/s^2$ (see Fig.3(a, b)).
- 2) **Oscillation signal:** The leader abruptly accelerates to $23.6 m/s$ within $12s$ and holds this velocity for $15s$. Then, the leader decelerates to $16.4 m/s$ over $12s$ and accelerates back to $20m/s$ in $12s$ (see Fig.3(c, d)).

TABLE I: Network and traffic simulation parameters.

Parameters	Value
Platoon size n	5 vehicles
Vehicle length L	5 [m]
Engine actuator delay τ_i	0.2 [s] ¹
Weight of edge (i, j) a_{ij}	$\frac{1}{d_i}$
Minimum communication delay h_m	0 [m]
Maximum communication delay h_M	0.3 [m]
Minimum communication delay slope d_m	-0.1
Maximum communication delay slope d_M	0.1

¹ [75, 76]

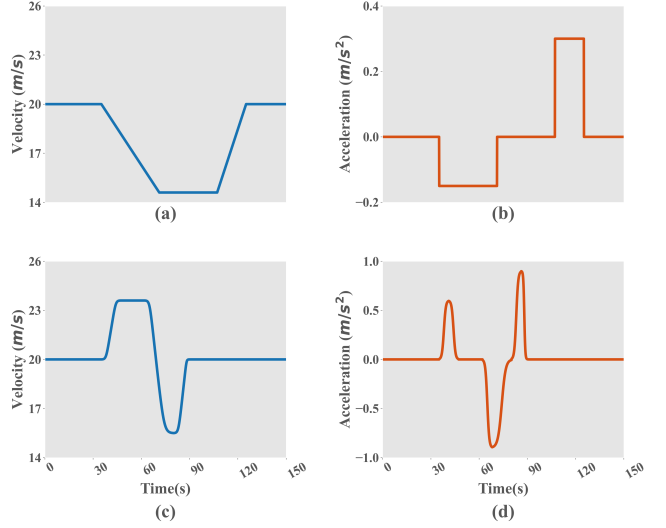


Fig. 3: The two representative leader maneuvers: (a) and (b) denotes the velocity and acceleration of the trapezoidal signal, respectively; (c) and (d) denote the velocity and acceleration of the oscillation signal, respectively.

B. Numerical analyses of the CAV platoon under the PLF

In this subsection, the analysis concentrates on the CAV platoon that employs the PLF, using the same control parameters for each CAV in the platoon, in accordance with the conditions of Theorem 8. The influence of tracking performance with varying feedback control gains is explored by selecting four feedback control gains:

- 1) *Parameter I:* $k_i = [0.3, 0.3, 0.3]^T$;
- 2) *Parameter II:* $k_i = [1, 0.3, 0.3]^T$;
- 3) *Parameter III:* $k_i = [0.3, 1, 0.3]^T$;
- 4) *Parameter IV:* $k_i = [0.3, 0.3, 1]^T$.

Furthermore, the desired time headway is set to $h_i = 0.6s$ [77, 78]. The corresponding matrices P, S, Q, R , and X are provided in Appendix C. A detailed analysis is conducted on the tracking performance and safety conditions.

1) **Tracking performance analyses:** Upon the formation of the CAV platoon and reaching the equilibrium state where the tracking error is zero, the tracking performance of the four feedback control gains under investigation is assessed using the trapezoidal signal depicted in Fig.3(a,b) as the leader maneuver. The results are presented in Fig.4, which illustrates

the tracking of the leader motion by the various CAVs in the platoon.

As anticipated from the theoretical outcomes, all CAVs can smoothly track the leader motion with a steady-state error of 0. Transient variations in the leader motion can provoke abrupt changes in the tracking error, which decrease over time due to stability. Moreover, the impact of different feedback control gains on the tracking performance varies, as demonstrated by comparing the results of the four control gains. Elevating the gain of the spacing and velocity errors significantly diminishes the overshoot of the acceleration curve, particularly in the case of the velocity error gain, where the overshoot is effectively suppressed. However, augmenting the gain of the spacing error results in oscillations in the acceleration curve, potentially owing to time-varying delay. Conversely, increasing the gain of the acceleration error adversely affects the tracking performance because of dramatic fluctuations, even though stability is maintained. Consequently, regarding control parameter selection, enhancing the gain of the velocity error within an appropriate range can improve the tracking performance to some extent.

Moreover, the tracking performance of the four feedback control gains is assessed under the oscillation signal presented in Fig.3(c, d). Fig.5 displays the corresponding tracking performance for the four feedback control gains. Under the oscillation signal, all cases with the four feedback control gains maintain excellent tracking performance, with each vehicle adjusting to changes in leader motion and returning to the equilibrium state with zero steady-state error. A similar phenomenon and conclusion as in Fig.4 can be observed, indicating that increasing the gain of spacing and velocity errors can benefit tracking performance, while increasing the gain of acceleration errors does not necessarily provide the same benefits.

Additionally, to complement the analysis on stability through tracking performance, two widely accepted indicators, namely Setting Time (ST) and Number of Oscillations (NOO), are employed for evaluating the transient response performance of different feedback control gains [79, 80]. ST is defined as "the time required for the response curve to reach and stay within a range of a certain percentage (2%) of the final value," while NOO is "the number of deviations of the response curve from the final value caused by errors in the setting time." Both ST and NOO are crucial measures of transient response, with ST representing the speed of achieving equilibrium and NOO representing the accuracy and comfort of the response. Since the investigation focuses on the differences in the transient response of various feedback control gains, the form of leader motion has little impact, and thus the results are analyzed here only for the Trapezoidal signal case.

Fig.6 compares the effects of different feedback control gains on two transient response indicators: Setting time (ST) and Number of oscillations (NOO). The results indicate that different control gains have a significant impact on transient response. Specifically, Parameter II and Parameter III show smaller ST and NOO than Parameter I, indicating that increasing the gain of spacing and velocity errors is effective

in reducing velocity fluctuations and time from perturbation to equilibrium, thereby improving driving comfort and safety. However, increasing the gain of acceleration error, as in Parameter IV, does not improve transient response. Moreover, for all control gain cases, the ST increases and NOO decreases with increasing vehicle index, suggesting that larger CAV platoons have less velocity fluctuation from perturbation to equilibrium, albeit with longer recovery times. Notably, Parameter III results in NOO=0, indicating no overshoot during transient response, and thus, performs well in terms of safety and comfort.

2) *Safety analyses considering hard braking maneuver:* To further assess safety across various driving scenarios and feedback control gains, we conduct a quantitative analysis to examine the potential emergence of critical driving situations for all feedback control gains under investigation. This analysis utilizes the well-established safety indicator, Deceleration Rate to Avoid the Crash (DRAC), which has been extensively studied in the literature [81, 82]. This indicator presents the deceleration rate needed to be applied by a vehicle to avoid a collision with another vehicle which can be defined for each vehicle i at the time t as follows:

$$DRAC_i(t) = \frac{(v_i(t) - v_{i-1}(t))^2}{2(p_{i-1}(t) - p_i(t) - L)}. \quad (34)$$

Furthermore, an additional scenario was considered to evaluate safety across various driving scenarios and feedback control gains, specifically a hard braking maneuver where the Leader decelerates from 20m/s to 0m/s within 20s. The reaction of the CAV platoon to this scenario for the four feedback control gains under investigation is displayed in Fig.7. Notably, the CAVs in the platoon accurately track the Leader motion and decelerate to 0m/s without collision under each control gain. The DRAC of different CAVs under different control gains in the hard braking maneuver is presented as boxplots in Fig.8, with the Leader's DRAC omitted due to its lack of a predecessor. The second through fifth CAVs in the platoon are denoted as CAV2, CAV3, CAV4, and CAV5, respectively.

From Fig.8, a notable phenomenon can be observed by comparing the boxplots. The median DRAC of all CAVs under Parameter II and Parameter III is significantly lower than that under Parameter I and Parameter IV, which is consistent with the rough results obtained in the tracking performance analyses. This finding suggests that increasing the gain of spacing and velocity errors can maintain better safety compared to increasing the gain of acceleration error. Furthermore, a second conclusion can be drawn by comparing different CAVs under the same feedback control gain. Despite the control parameters being identical, the position of a CAV in the platoon influences the safety conditions.

C. Numerical analyses of the alternative IFTs

In this subsection, the parameters in Table I are still adopted for both network and traffic simulation. Moreover, the control parameters are set to $k_i = [0.3, 0.3, 0.3]^T$ and $h_i = 0.6s$. The difference is that the section mainly analyzes the tracking performance of the CAV platoon employed by PF, BD or BDL. It is worth mentioning that the control parameters chosen here

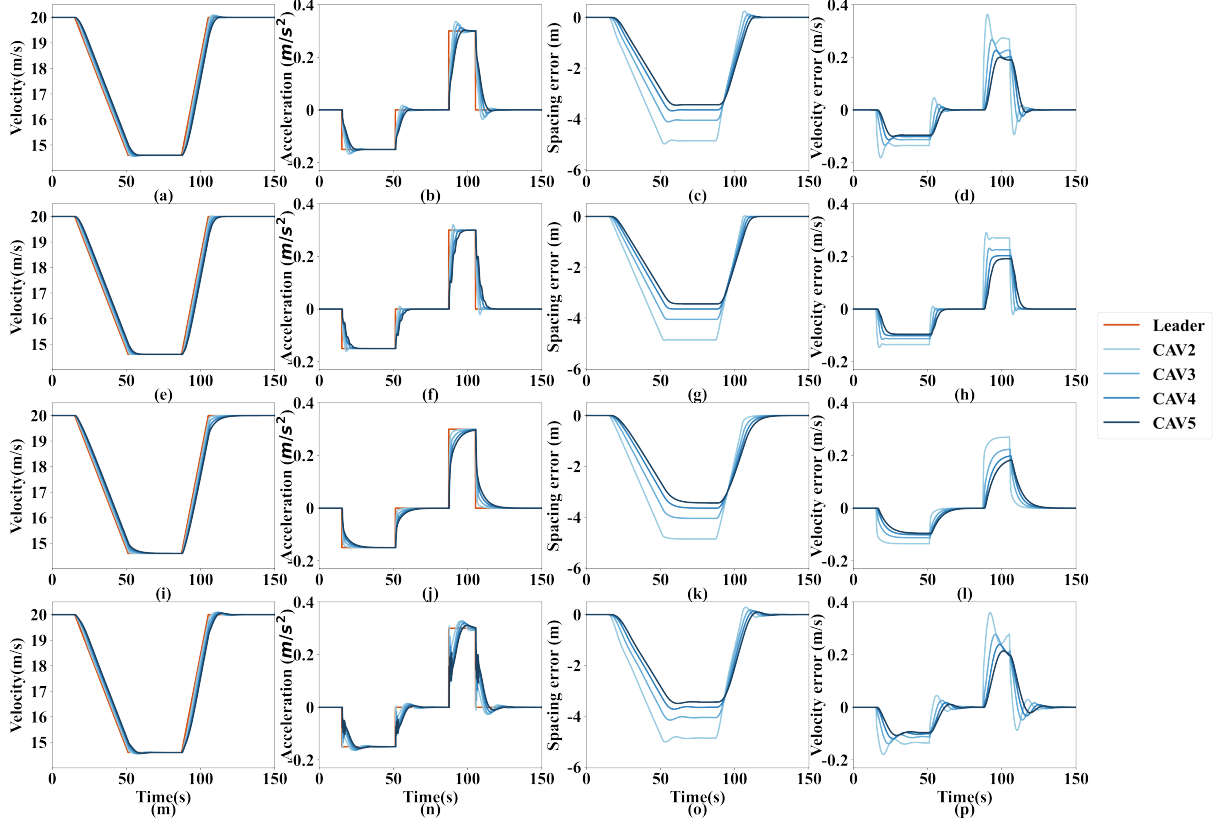


Fig. 4: The tracking performance of the CAV platoon for the Trapezoidal signal in Fig. 3(a,b) under the four feedback control gains is as follows: (a), (b), (c), and (d) display the tracking results under Parameter I, including the velocity, acceleration, tracking error of spacing, and tracking error of velocity, respectively; (e), (f), (g), and (h) depict the case under Parameter II; (i), (j), (k), and (l) represent the case under Parameter III; (m), (n), (o), and (p) illustrate the case under Parameter IV.

still exist matrixes P, S, Q, R , and X satisfy the Theorem 8, which can be found in Appendix C.

As in Section IV-B1, the Trapezoidal signal defined in Section IV-A is employed to investigate the tracking performance of different IFTs. The tracking performance of the CAV platoon is presented in Fig.9.

Alternative IFTs have also been evaluated, and they have demonstrated favorable tracking performance. A similar phenomenon can be observed, where the transient response from tracking Leader motion decreases gradually, thanks to stability. It is worth noting that for the cases of BD and BDL, the tracking process is smooth; on the contrary, there are significant fluctuations in the tracking process for the case of PF, as disclosed in the recent technical literature [83].

Similarly, ST and NOO are analyzed to investigate the specific effects of different IFTs on the transient response, and the results are demonstrated in Fig.10. It can be found that the case under BD has a significantly higher ST than the cases under the other three IFTs. Moreover, although the ST of the cases under all IFTs increases with the increase of the vehicle index, only the case under PF increases significantly while the cases under the other IFTs increase very slightly. One conclusion can be drawn that the CAV platoon with PLF and BDL recovers from the perturbation to the equilibrium state more quickly than PF and BD. In fact, this phenomenon

arises due to the direct communication with the leader, which effectively mitigates hard oscillations during transients.

On the other hand, as the vehicle index increases, for the cases under PLF, BD, and BDL, the NOO decreases, while for the cases under PF, the NOO increases. Furthermore, of the other three IFTs, the case under BD has the largest NOO, and the case under BDL has the smallest. In general, the transient performance can be significantly enhanced by communicating with the leader and bi-directional communication.

V. CONCLUSION AND FUTURE WORK

In this paper, we propose a general supermatrix modeling approach for the CAV platoon, taking into account time-varying communication delays. Communication relationships within a CAV platoon, typically defined by IFT, are described using graph theory. The linear time-invariant state time-varying delay system corresponding to the CAV platoon employing a CTH control strategy is modeled using supermatrices. By applying the Wirtinger-Based Integral Inequality and Lyapunov-Krasovskii Stability Theorem, a novel stability condition for the general CAV platoon is derived, based on the properties of the linear time-invariant state time-varying delay system. Moreover, extensive numerical analyses are conducted to thoroughly assess the tracking performance and safety conditions of four control parameters, offering guidance for

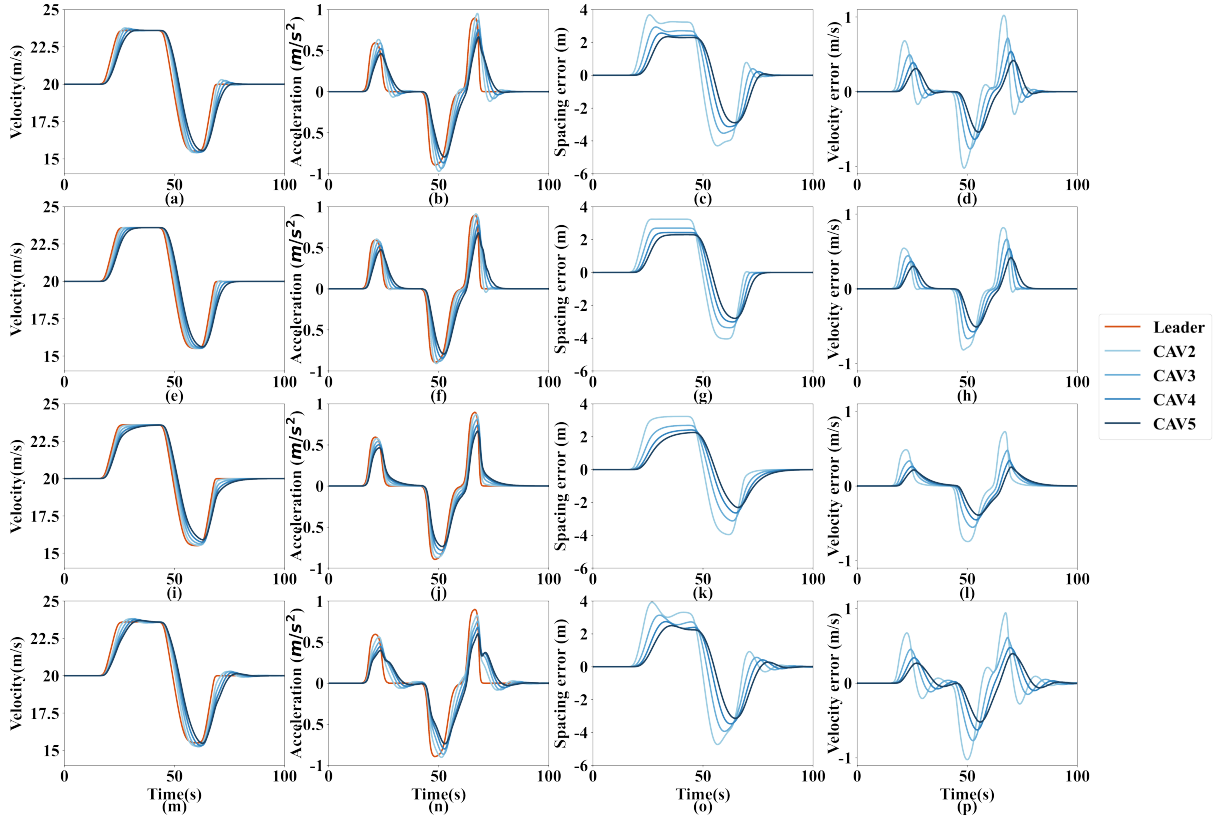


Fig. 5: The tracking performance of the CAV platoon for the Oscillation signal in Fig. 3(c,d) under the four feedback control gains is as follows: (a), (b), (c), and (d) display the tracking results under Parameter I, including the velocity, acceleration, tracking error of spacing, and tracking error of velocity, respectively; (e), (f), (g), and (h) depict the case under Parameter II; (i), (j), (k), and (l) represent the case under Parameter III; (m), (n), (o), and (p) illustrate the case under Parameter IV.

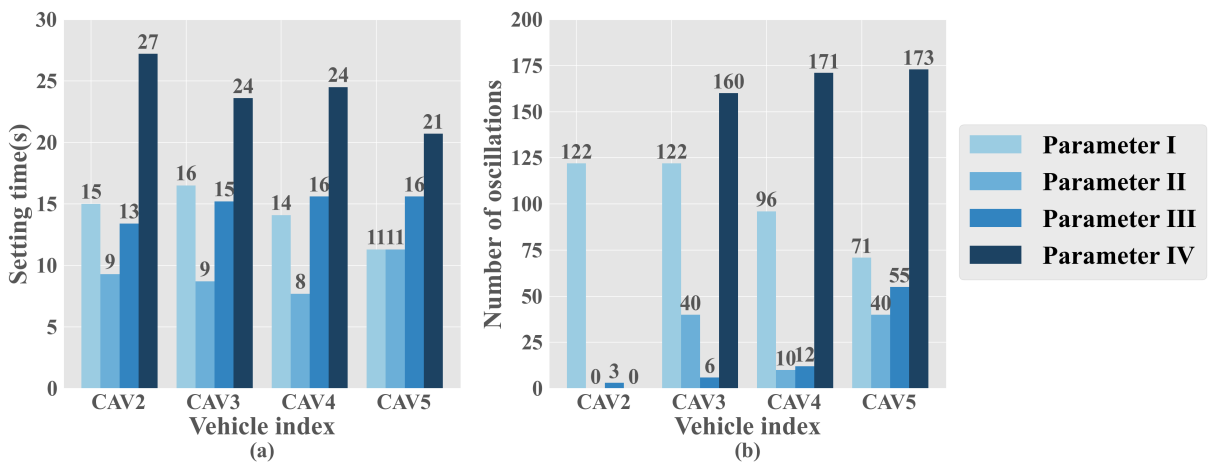


Fig. 6: Indicators for evaluating the transient response of each CAV within the CAV platoon under the four feedback control gains: (a) the case of setting time; (b) the case of the number of oscillations.

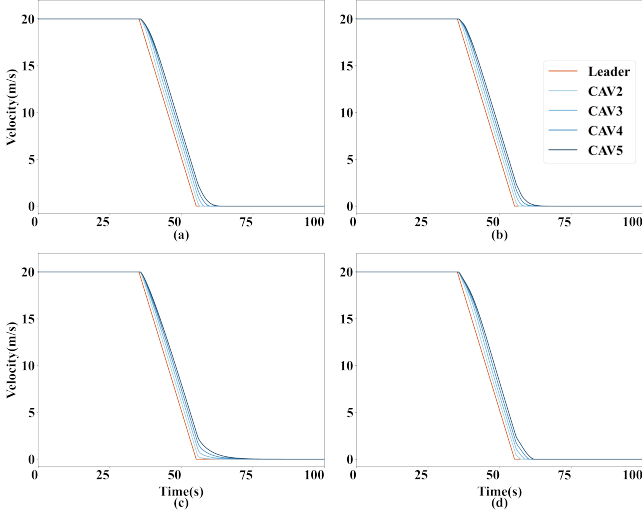


Fig. 7: The tracking performance for a hard braking maneuver for each feedback control gain under investigation: (a) Parameter I; (b) Parameter II; (c) Parameter III; (d) Parameter IV.

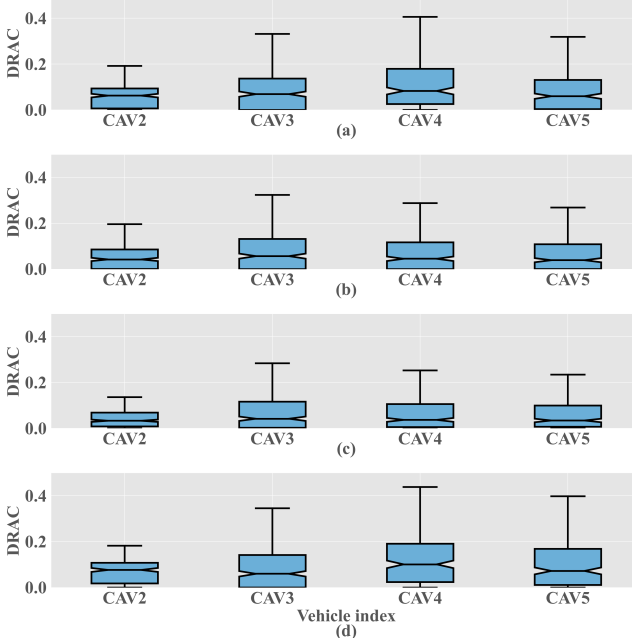


Fig. 8: The DRAC boxplots for each CAV of each feedback control gain under investigation: (a) Parameter I; (b) Parameter II; (c) Parameter III; (d) Parameter IV.

selecting control parameters. Finally, we present a comparison of tracking performance between CAV platoons employing different IFTs, providing insights into IFT selection.

The theoretical and numerical analysis leads us to the following conclusions:

- 1) A stability condition considering time-varying delay for the CAV platoon can be obtained using the Lyapunov-Krasovskii Stability Theorem and Wirtinger-Based Integral Inequality.
- 2) The CAV platoon, using the investigated control parameters and IFTs, can smoothly track leader motion, maintain

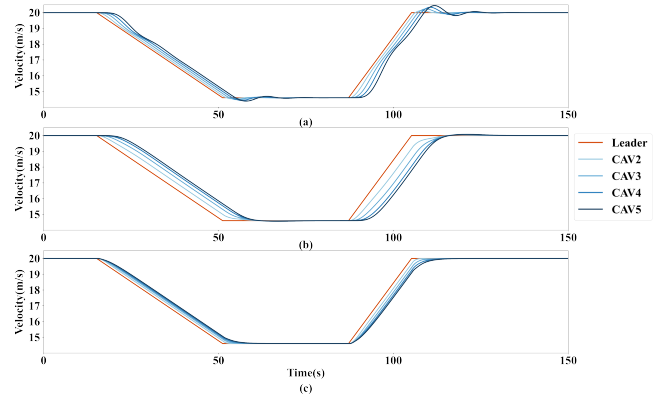


Fig. 9: Tracking performance of the CAV platoon for the Trapezoidal signal in Fig. 3(a,b) under the alternative three IFTs: (a) presents tracking results under PF; (b) presents tracking results under BD; (c) denotes the case under BDL.

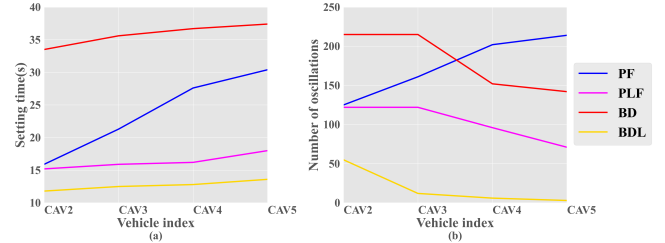


Fig. 10: Indicators for evaluating the transient response of each CAV among the CAV platoon under the four IFTs: (a) the case of setting time; (b) the case of the number of oscillations.

- safe conditions in various scenarios, and ensure stability.
- 3) Both tracking performance and safety conditions benefit from increasing the gain of spacing and velocity errors, while increasing the gain of acceleration errors does not.
 - 4) Communication with the leader and bi-directional communication can significantly enhance tracking and transient performance from an IFT perspective.

However, we recognize that the vehicle behavior in the simulation is a simplification of reality, and additional field experiments are required to provide a more accurate analysis of tracking performance. Similarly, the time-varying delay function used in this paper, an assumed Bessel function that satisfies the condition of both the delay and its derivative being bounded, does not perfectly fit the actual time-varying delay. Hence, corresponding field experiments should be conducted to gain insights into the time-varying relationship of communication delays. Furthermore, future research should focus on investigating the control parameter scheme yielding optimal tracking performance through theoretical research and field experiments and designing novel control strategies to enable smoother and safer tracking performance.

APPENDIX

APPENDIX A. FEEDBACK CONTROL FOR LINEARIZATION

In this appendix, we provide the linearization of the longitudinal vehicle dynamic in Equation (1). The functions of the

lumped uncertain resistance forces, including $f_i^g(t)$, $f_i^w(t)$, and $f_i^r(t)$ are expressed as follows:

$$\begin{cases} f_i^g(t) = m_i g \sin(\theta_i(t)), \\ f_i^w(t) = \frac{1}{2} \rho C_D A_F (v_i(t) + v_w(t))^2, \\ f_i^r(t) = \mu_R m_i g \cos(\theta_i(t)). \end{cases} \quad (35)$$

where $g = 9.81 \text{m/s}^2$ denotes the acceleration of gravity; $\theta_i(t)$ is the inclination angle of the road; ρ denotes the air density; C_D is the aerodynamic drag coefficient; A_F represents the maximal cross-sectional/frontal area of the vehicle; $v_w(t)$ denotes the uncertain headwind speed; μ_R is the coefficient of rolling resistance.

The desired engine dynamic is modeled as follows:

$$(\tau_i s + 1) F_i^e = U_i. \quad (36)$$

Adopting the inverse Laplace transformation on Equation (36) arrives at:

$$\dot{f}_i^e(t) = \frac{u_i(t)}{\tau_i} - \frac{f_i^e(t)}{\tau_i}. \quad (37)$$

Substituting Equation (1) into Equation (37) and differentiating both sides of Equation (37) with respect to time, we get:

$$\begin{aligned} \dot{a}_i(t) &= \frac{\dot{f}_i^e(t)}{m_i} - \frac{\dot{f}_i^g(t)}{m_i} - \frac{\dot{f}_i^{i\omega}(t)}{m_i} - \frac{\dot{f}_i^r(t)}{m_i} \\ &= \frac{u_i(t)}{m_i \tau_i} \\ &\quad - \frac{a_i(t) + g \sin(\theta_i(t)) [1 - \tau_i \mu_R \dot{\theta}_i(t)] + g \cos(\theta_i(t)) [1 + \tau_i \dot{\theta}_i(t)]}{\tau_i} \\ &\quad - \frac{\frac{1}{2} \rho C_D A_F (v_i(t) + v_w(t)) ((v_i(t) + v_w(t)) + 2\tau_i (a_i(t) + \dot{v}_w(t)))}{\tau_i}. \end{aligned} \quad (38)$$

Thus, the nonlinear state feedback chosen for linearizing can be defined by:

$$\begin{aligned} u_i^*(t) &= m_i u_i(t) + g \sin(\theta_i(t)) [1 - \tau_i \mu_R \dot{\theta}_i(t)] \\ &\quad + g \cos(\theta_i(t)) [1 + \tau_i \dot{\theta}_i(t)] \\ &\quad + \frac{1}{2} \rho C_D A_F (v_i(t) + v_w(t)) \\ &\quad ((v_i(t) + v_w(t)) + 2\tau_i (a_i(t) + \dot{v}_w(t))). \end{aligned} \quad (39)$$

Under the new feedback control input, the Equation (1) can be rewritten as:

$$\tau_i \dot{a}_i(t) + a_i(t) = u_i(t). \quad (40)$$

APPENDIX B. CONNECTION BETWEEN LYAPUNOV-KRASOVSKII STABILITY THEOREM AND SECOND LYAPUNOV METHOD.

First, we present a lemma on the Lyapunov function:

Lemma 11. ([84]) Let a system $\dot{X}(t) = f(X(t), X(t-h(t)))$ with $f(0,0) = 0$. Assume the Lyapunov function $F : G \rightarrow \mathbb{R}$ exists with $X, y \in G$, $F(y) < F(X)$ implies

$$(\dot{F}(X) f(X, y)) (\dot{F}(X) f(X, y)) \leq 0. \quad (41)$$

Then the solution $X(t) \equiv 0$ is stable.

Suppose there exists a Lyapunov function $F : \mathbb{R}^n \rightarrow \mathbb{R}$. Then define functional $V : C \rightarrow \mathbb{R}$ as follows:

$$V(\phi) := \max_{-h \leq \theta \leq 0} F(\phi(\theta)), (\forall \phi \in C). \quad (42)$$

By definition, the following conditions hold:

$$\dot{V}(\phi) \begin{cases} \leq 0, & \text{if } F(\phi(0)) < V(\phi), \\ = \max(\dot{F}(\phi(0)), f(\phi(0), \phi(-h(t))), 0), & \text{if } F(\phi(0)) = V(\phi), \end{cases} \quad (43)$$

where $f(\phi(0), \phi(-h(t))) = \Psi\phi(0) + \Psi_d\phi(-h(t))$.

Thus $\dot{V}(\phi) > 0$ holds if and only if the following condition holds:

$$F(\phi(0)) = \max_{-h \leq \theta \leq 0} F(\phi(\theta)) \text{ and } (\dot{F}(\phi(0)), f(\phi(0), \phi(-h(t)))) > 0. \quad (44)$$

The function F can be defined in some neighborhood $G \subset \mathbb{R}^n$. And the functional V is then defined for $\phi \in C$ with values in G .

Suppose Equation (44) holds for some functions $\phi \in C$, then we can obtain the inequality $F(\phi(-h(t))) < F(\phi(0))$ making ϕ arbitrarily small. Thus the second condition in Equation (44) still holds, but conflicts with Lemma 11. Therefore $\dot{V}(\phi) \leq 0$ holds constantly for all ϕ .

It can be concluded that the Lyapunov-Krasovskii Stability Theorem can be considered as an extension of the Second Lyapunov method to functional space. This extension does not introduce any additional constraints since it only constrains the definite sign at the start and end points instead of in the neighborhood. As a result, the stability conditions obtained using the Lyapunov-Krasovskii Stability Theorem are more accurate than those obtained using the Second Lyapunov method. This conclusion has been supported by previous research [44, 45].

APPENDIX C. ATTACHMENTS UPLOADED TO GITHUB

The uploaded code for this paper includes the formulation of Theorem 1 and the construction of LMIs for Theorem 8. Additionally, matrices corresponding to the four sets of control parameters for PLF, as selected in Section IV-B, and three sets for PF, BD, and BDL, as selected in Section IV-C, which are compatible with Theorem 8, have been included in the repository. The file repository URL is: <https://github.com/ruantiancheng/code-of-paper8>.

ACKNOWLEDGMENT

This research was sponsored by the National Key Research and Development Program of China (No. 2022ZD0115600), National Science Foundation of China (No. 52072067), Post-graduate Research & Practice Innovation Program of Jiangsu Province (KYCX22_0266), and Natural Science Foundation of Jiangsu Province (No. BK20210249).

REFERENCES

- [1] D. Schrank, B. Eisele, and T. Lomax, “Urban mobility report 2019,” 2019, publisher: Texas Transportation Institute.
- [2] I. G. Jin and G. Orosz, “Optimal control of connected vehicle systems with communication delay and driver

- reaction time,” *IEEE Transactions on Intelligent Transportation Systems*, vol. 18, no. 8, pp. 2056–2070, 2016.
- [3] T. Ruan, H. Wang, L. Zhou, Y. Zhang, C. Dong, and Z. Zuo, “Impacts of Information Flow Topology on Traffic Dynamics of CAV-MV Heterogeneous Flow,” *IEEE Transactions on Intelligent Transportation Systems*, pp. 1–16, 2022.
- [4] J. F. Gilmore and N. Abe, “Neural network models for traffic control and congestion prediction,” *Journal of Intelligent Transportation Systems*, vol. 2, no. 3, pp. 231–252, 1995.
- [5] A. A. Kurzhanskiy and P. Varaiya, “Traffic management: An outlook,” *Economics of transportation*, vol. 4, no. 3, pp. 135–146, 2015.
- [6] Z. Zhong, E. E. Lee, M. Nejad, and J. Lee, “Influence of CAV clustering strategies on mixed traffic flow characteristics: An analysis of vehicle trajectory data,” *Transportation Research Part C: Emerging Technologies*, vol. 115, p. 102611, 2020.
- [7] B. van Arem, M. M. Abbas, X. Li, L. Head, X. Zhou, D. Chen, R. Bertini, S. P. Mattingly, H. Wang, and G. Orosz, “Integrated traffic flow models and analysis for automated vehicles,” in *Road Vehicle Automation 3*. Springer, 2016, pp. 249–258.
- [8] L. Ye and T. Yamamoto, “Impact of dedicated lanes for connected and autonomous vehicle on traffic flow throughput,” *Physica A: Statistical Mechanics and its Applications*, vol. 512, pp. 588–597, 2018.
- [9] T. Ruan, L. Zhou, and H. Wang, “Stability of heterogeneous traffic considering impacts of platoon management with multiple time delays,” *Physica A: Statistical Mechanics and its Applications*, vol. 583, p. 126294, 2021.
- [10] S. Ulbrich, A. Reschka, J. Rieken, S. Ernst, G. Bagschik, F. Dierkes, M. Nolte, and M. Maurer, “Towards a functional system architecture for automated vehicles,” *arXiv preprint arXiv:1703.08557*, 2017.
- [11] R. E. Wilson and J. A. Ward, “Car-following models: Fifty years of linear stability analysis - a mathematical perspective,” *Transportation Planning and Technology*, vol. 34, no. 1, pp. 3–18, 2011.
- [12] R. E. Wilson, “Mechanisms for spatio-temporal pattern formation in highway traffic models,” *Philosophical Transactions of the Royal Society A: Mathematical, Physical and Engineering Sciences*, vol. 366, no. 1872, pp. 2017–2032, 2008, publisher: The Royal Society London.
- [13] B. Goñi-Ros, W. J. Schakel, A. E. Papacharalampous, M. Wang, V. L. Knoop, I. Sakata, B. van Arem, and S. P. Hoogendoorn, “Using advanced adaptive cruise control systems to reduce congestion at sags: An evaluation based on microscopic traffic simulation,” *Transportation Research Part C: Emerging Technologies*, vol. 102, pp. 411–426, 2019, publisher: Elsevier.
- [14] I. K. Nikolos, A. I. Delis, and M. Papageorgiou, “Macroscopic Modelling and Simulation of ACC and CACC Traffic,” in *IEEE Conference on Intelligent Transportation Systems, Proceedings, ITSC*, vol. 2015-Octob. IEEE, 2015, pp. 2129–2134.
- [15] A. Kesting, M. Treiber, and D. Helbing, “Enhanced intelligent driver model to access the impact of driving strategies on traffic capacity,” *Philosophical Transactions of the Royal Society A: Mathematical, Physical and Engineering Sciences*, vol. 368, no. 1928, pp. 4585–4605, 2010, publisher: The Royal Society Publishing.
- [16] F. Navas and V. Milanés, “Mixing V2V- and non-V2V-equipped vehicles in car following,” *Transportation Research Part C: Emerging Technologies*, vol. 108, no. September, pp. 167–181, 2019. [Online]. Available: <https://doi.org/10.1016/j.trc.2019.08.021>
- [17] L. Zhou, T. Ruan, K. Ma, C. Dong, and H. Wang, “Impact of CAV platoon management on traffic flow considering degradation of control mode,” *Physica A: Statistical Mechanics and its Applications*, vol. 581, p. 126193, 2021.
- [18] K. C. Dey, L. Yan, X. Wang, Y. Wang, H. Shen, M. Chowdhury, L. Yu, C. Qiu, and V. Soundararaj, “A review of communication, driver characteristics, and controls aspects of cooperative adaptive cruise control (CACC),” *IEEE Transactions on Intelligent Transportation Systems*, vol. 17, no. 2, pp. 491–509, 2015.
- [19] Y. Zheng, S. E. Li, K. Li, and L.-Y. Wang, “Stability margin improvement of vehicular platoon considering undirected topology and asymmetric control,” *IEEE Transactions on Control Systems Technology*, vol. 24, no. 4, pp. 1253–1265, 2015, publisher: IEEE.
- [20] A. Ghiasi, O. Hussain, Z. S. Qian, and X. Li, “A mixed traffic capacity analysis and lane management model for connected automated vehicles: A Markov chain method,” *Transportation Research Part B: Methodological*, vol. 106, pp. 266–292, 2017.
- [21] Y. Li, Z. Chen, Y. Yin, and S. Peeta, “Deployment of roadside units to overcome connectivity gap in transportation networks with mixed traffic,” *Transportation Research Part C: Emerging Technologies*, vol. 111, pp. 496–512, 2020, publisher: Elsevier.
- [22] M. Sala and F. Sorriguera, “Capacity of a freeway lane with platoons of autonomous vehicles mixed with regular traffic,” *Transportation research part B: methodological*, vol. 147, pp. 116–131, 2021, publisher: Elsevier.
- [23] X. Chang, H. Li, J. Rong, and X. Zhao, “Analysis on traffic stability and capacity for mixed traffic flow with platoons of intelligent connected vehicles,” *Physica A: Statistical Mechanics and its Applications*, vol. 557, p. 124829, 2020.
- [24] Y. Zhou, M. Wang, and S. Ahn, “Distributed model predictive control approach for cooperative car-following with guaranteed local and string stability,” *Transportation research part B: methodological*, vol. 128, pp. 69–86, 2019.
- [25] M. Montanino and V. Punzo, “On string stability of a mixed and heterogeneous traffic flow: A unifying modelling framework,” *Transportation Research Part B: Methodological*, vol. 144, pp. 133–154, 2021.
- [26] W. Yu, X. Hua, and W. Wang, “Investigating the longitudinal impact of cooperative adaptive cruise control vehicle degradation under communication interruption,” *IEEE Intelligent Transportation Systems Magazine*, 2021.

- [27] H. Liu, X. Kan, S. E. Shladover, X.-Y. Lu, and R. E. Ferlis, "Impact of cooperative adaptive cruise control on multilane freeway merge capacity," *Journal of Intelligent Transportation Systems*, vol. 22, no. 3, pp. 263–275, 2018.
- [28] L. Xiao, M. Wang, W. Schakel, and B. van Arem, "Unravelling effects of cooperative adaptive cruise control deactivation on traffic flow characteristics at merging bottlenecks," *Transportation research part C: emerging technologies*, vol. 96, pp. 380–397, 2018.
- [29] G. Orosz, "Connected cruise control: modelling, delay effects, and nonlinear behaviour," *Vehicle System Dynamics*, vol. 54, no. 8, pp. 1147–1176, 2016.
- [30] J. C. Doyle, B. A. Francis, and A. R. Tannenbaum, *Feedback control theory*. Courier Corporation, 2013.
- [31] R. Sipahi, S.-I. Niculescu, C. T. Abdallah, W. Michiels, and K. Gu, "Stability and stabilization of systems with time delay," *IEEE Control Systems Magazine*, vol. 31, no. 1, pp. 38–65, 2011.
- [32] R. Herman, E. W. Montroll, R. B. Potts, and R. W. Rothery, "Traffic dynamics: analysis of stability in car following," *Operations research*, vol. 7, no. 1, pp. 86–106, 1959.
- [33] X. Zhang and D. F. Jarrett, "Stability analysis of the classical car-following model," *Transportation Research Part B: Methodological*, vol. 31, no. 6, pp. 441–462, 1997.
- [34] Y. Li, D. Sun, and M. Cui, "Lyapunov stability analysis for the full velocity difference car-following model," *Control Theory & Applications*, vol. 12, p. 014, 2010.
- [35] Y. Li, H. Zhu, M. Cen, Y. Li, R. Li, and D. Sun, "On the stability analysis of microscopic traffic car-following model: a case study," *Nonlinear Dynamics*, vol. 74, no. 1, pp. 335–343, 2013.
- [36] G. K. Kamath, K. Jagannathan, and G. Raina, "Car-following models with delayed feedback: local stability and hopf bifurcation," in *2015 53rd Annual Allerton Conference on Communication, Control, and Computing (Allerton)*. IEEE, 2015, pp. 538–545.
- [37] J. Sun, Z. Zheng, and J. Sun, "Stability analysis methods and their applicability to car-following models in conventional and connected environments," *Transportation research part B: methodological*, vol. 109, pp. 212–237, 2018, publisher: Elsevier.
- [38] W. B. Qin and G. Orosz, "Experimental validation of string stability for connected vehicles subject to information delay," *IEEE Transactions on Control Systems Technology*, vol. 28, no. 4, pp. 1203–1217, 2019.
- [39] L. Zhang, J. Sun, and G. Orosz, "Hierarchical design of connected cruise control in the presence of information delays and uncertain vehicle dynamics," *IEEE Transactions on Control Systems Technology*, vol. 26, no. 1, pp. 139–150, 2017.
- [40] H. Lhachemi and C. Prieur, "Feedback stabilization of a class of diagonal infinite-dimensional systems with delay boundary control," *IEEE Transactions on Automatic Control*, vol. 66, no. 1, pp. 105–120, 2020.
- [41] F. Gao, S. E. Li, Y. Zheng, and D. Kum, "Robust control of heterogeneous vehicular platoon with uncertain dynamics and communication delay," *IET Intelligent Transport Systems*, vol. 10, no. 7, pp. 503–513, 2016.
- [42] X.-Y. Guo, G. Zhang, and A.-F. Jia, "Stability and energy consumption of a double flow controlled two-lane traffic system with vehicle-to-infrastructure communication," *Applied Mathematical Modelling*, 2023.
- [43] E. Fridman, "Descriptor discretized lyapunov functional method: analysis and design," *IEEE Transactions on Automatic control*, vol. 51, no. 5, pp. 890–897, 2006.
- [44] Y. Wang, Y. Xia, and P. Zhou, "Fuzzy-model-based sampled-data control of chaotic systems: A fuzzy time-dependent lyapunov-krasovskii functional approach," *IEEE Transactions on fuzzy systems*, vol. 25, no. 6, pp. 1672–1684, 2016.
- [45] H.-H. Lian, S.-P. Xiao, H. Yan, F. Yang, and H.-B. Zeng, "Dissipativity analysis for neural networks with time-varying delays via a delay-product-type lyapunov functional approach," *IEEE transactions on neural networks and learning systems*, vol. 32, no. 3, pp. 975–984, 2020.
- [46] H. R. Feyzmahdavian, A. Alam, and A. Gattami, "Optimal distributed controller design with communication delays: Application to vehicle formations," in *2012 IEEE 51st IEEE Conference on Decision and Control (CDC)*. IEEE, 2012, pp. 2232–2237.
- [47] X. Liu, A. Goldsmith, S. S. Mahal, and J. K. Hedrick, "Effects of communication delay on string stability in vehicle platoons," in *ITSC 2001. 2001 IEEE Intelligent Transportation Systems. Proceedings (Cat. No. 01TH8585)*. IEEE, 2001, pp. 625–630.
- [48] M. Yang, B. Ai, R. He, Z. Zhong, R. Chen, and H. Zhang, "Time-varying characteristics for v2v channels in complicated scenarios," in *2021 XXXIVth General Assembly and Scientific Symposium of the International Union of Radio Science (URSI GASS)*. IEEE, 2021, pp. 1–4.
- [49] G. Fiengo, D. G. Lui, A. Petrucci, S. Santini, and M. Tufo, "Distributed robust pid control for leader tracking in uncertain connected ground vehicles with v2v communication delay," *IEEE/ASME Transactions on Mechatronics*, vol. 24, no. 3, pp. 1153–1165, 2019.
- [50] E. Louarroudi, J. Lataire, R. Pintelon, P. Janssens, and J. Swevers, "Frequency domain, parametric estimation of the evolution of the time-varying dynamics of periodically time-varying systems from noisy input–output observations," *Mechanical Systems and Signal Processing*, vol. 47, no. 1-2, pp. 151–174, 2014.
- [51] A. Otto, "Frequency domain methods for the analysis of time delay systems," 2016.
- [52] J. Reiner, G. J. Balas, and W. L. Garrard, "Flight control design using robust dynamic inversion and time-scale separation," *Automatica*, vol. 32, no. 11, pp. 1493–1504, 1996.
- [53] C. L. Shah, "On the modeling of time-varying delays," Ph.D. dissertation, Texas A&M University, 2004.
- [54] P. POPEO, "Federal communications commission," 2020.
- [55] L. L. C. Verizon North, "Federal Communications Commission," *Proceeding Number*, vol. 19, p. 354, 2020.
- [56] M. Wang, "Infrastructure assisted adaptive driving to

- stabilise heterogeneous vehicle strings,” *Transportation Research Part C: Emerging Technologies*, vol. 91, no. April 2017, pp. 276–295, 2018, publisher: Elsevier. [Online]. Available: <https://doi.org/10.1016/j.trc.2018.04.010>
- [57] D. Jia and D. Ngoduy, “Enhanced cooperative car-following traffic model with the combination of V2V and V2I communication,” *Transportation Research Part B: Methodological*, vol. 90, pp. 172–191, 2016, publisher: Elsevier.
- [58] V. Vukadinovic, K. Bakowski, P. Marsch, I. D. Garcia, H. Xu, M. Sybis, P. Sroka, K. Wesolowski, D. Lister, and I. Thibault, “3GPP C-V2X and IEEE 802.11p for Vehicle-to-Vehicle communications in highway platooning scenarios,” *Ad Hoc Networks*, vol. 74, pp. 17–29, 2018.
- [59] H. V. Vu, Z. Liu, D. H. N. Nguyen, R. Morawski, and T. Le-Ngoc, “Multi-agent reinforcement learning for joint channel assignment and power allocation in platoon-based C-V2X systems,” *arXiv preprint arXiv:2011.04555*, 2020.
- [60] D. Martín-Sacristán, S. Roger, D. García-Roger, J. F. Monserrat, P. Spapis, C. Zhou, and A. Kaloxyllos, “Low-Latency Infrastructure-Based Cellular V2V Communications for Multi-Operator Environments With Regional Split,” *IEEE Transactions on Intelligent Transportation Systems*, vol. 22, no. 2, pp. 1052–1067, 2020.
- [61] M. Pirani, S. Baldi, and K. H. Johansson, “Impact of Network Topology on the Resilience of Vehicle Platoons,” *IEEE Transactions on Intelligent Transportation Systems*, 2022.
- [62] K. Gu, J. Chen, and V. L. Kharitonov, *Stability of time-delay systems*. Springer Science & Business Media, 2003.
- [63] K. Gu and Y. Liu, “Lyapunov–Krasovskii functional for uniform stability of coupled differential-functional equations,” *Automatica*, vol. 45, no. 3, pp. 798–804, 2009.
- [64] A. A. Martyniuk and R. Gutovski, “Integral inequalities and stability of motion,” *Kiev Izdatel Naukova Dumka*, 1979.
- [65] C.-K. Zhang, Y. He, L. Jiang, M. Wu, and H.-B. Zeng, “Stability analysis of systems with time-varying delay via relaxed integral inequalities,” *Systems & Control Letters*, vol. 92, pp. 52–61, 2016, publisher: Elsevier.
- [66] D. Li, Q. Liu, and X. Ju, “Uniform decay estimates for solutions of a class of retarded integral inequalities,” *Journal of Differential Equations*, vol. 271, pp. 1–38, 2021, publisher: Elsevier.
- [67] S. Saravanan, M. Syed Ali, G. Rajchakit, B. Hamachukiattikul, B. Priya, and G. K. Thakur, “Finite-time stability analysis of switched genetic regulatory networks with time-varying delays via Wirtinger’s integral inequality,” *Complexity*, vol. 2021, 2021, publisher: Hindawi.
- [68] R. Suresh and A. Manivannan, “Robust stability analysis of delayed stochastic neural networks via Wirtinger-based integral inequality,” *Neural Computation*, vol. 33, no. 1, pp. 227–243, 2021, publisher: MIT Press One Rogers Street, Cambridge, MA 02142-1209, USA journals-info
- [69] M. Park, O. Kwon, J. H. Park, S. Lee, and E. Cha, “Stability of time-delay systems via Wirtinger-based double integral inequality,” *Automatica*, vol. 55, pp. 204–208, 2015, publisher: Elsevier.
- [70] P. Park, J. W. Ko, and C. Jeong, “Reciprocally convex approach to stability of systems with time-varying delays,” *Automatica*, vol. 47, no. 1, pp. 235–238, 2011, publisher: Elsevier.
- [71] P. Pepe and Z.-P. Jiang, “A Lyapunov–Krasovskii methodology for ISS and iISS of time-delay systems,” *Systems & Control Letters*, vol. 55, no. 12, pp. 1006–1014, 2006, publisher: Elsevier.
- [72] L. Liang, J. Kim, S. C. Jha, K. Sivanesan, and G. Y. Li, “Spectrum and power allocation for vehicular communications with delayed csi feedback,” *IEEE Wireless Communications Letters*, vol. 6, no. 4, pp. 458–461, 2017.
- [73] B. Soret, M. C. Aguayo-Torres, and J. T. Entrambasaguas, “Capacity with explicit delay guarantees for generic sources over correlated rayleigh channel,” *IEEE Transactions on Wireless Communications*, vol. 9, no. 6, pp. 1901–1911, 2010.
- [74] J. L. Vicario and C. Anton-Haro, “Analytical assessment of multi-user vs. spatial diversity trade-offs with delayed channel state information,” *IEEE Communications Letters*, vol. 10, no. 8, pp. 588–590, 2006.
- [75] M. Wang, S. P. Hoogendoorn, W. Daamen, B. van Arem, B. Shyrokau, and R. Happee, “Delay-compensating strategy to enhance string stability of adaptive cruise controlled vehicles,” *Transportmetrica B*, vol. 6, no. 3, pp. 211–229, 2018. [Online]. Available: <https://doi.org/10.1080/21680566.2016.1266973>
- [76] Y. Zhou, S. Ahn, M. Wang, and S. Hoogendoorn, “Stabilizing mixed vehicular platoons with connected automated vehicles: An H-infinity approach,” *Transportation Research Part B: Methodological*, vol. 132, pp. 152–170, 2020.
- [77] Y. Li, H. Wang, W. Wang, L. Xing, S. Liu, and X. Wei, “Evaluation of the impacts of cooperative adaptive cruise control on reducing rear-end collision risks on freeways,” *Accident Analysis & Prevention*, vol. 98, pp. 87–95, 2017.
- [78] J. Ploeg, A. F. Serrarens, and G. J. Heijenk, “Connect & drive: design and evaluation of cooperative adaptive cruise control for congestion reduction,” *Journal of Modern Transportation*, vol. 19, pp. 207–213, 2011.
- [79] S. Bennett, *A history of control engineering, 1930-1955*. IET, 1993, no. 47.
- [80] E. D. Sontag, *Mathematical control theory: deterministic finite dimensional systems*. Springer Science & Business Media, 2013, vol. 6.
- [81] C. Fu and T. Sayed, “Comparison of threshold determination methods for the deceleration rate to avoid a crash (drac)-based crash estimation,” *Accident Analysis & Prevention*, vol. 153, p. 106051, 2021.
- [82] ———, “Random parameters bayesian hierarchical modeling of traffic conflict extremes for crash estimation,”

- Accident Analysis & Prevention*, vol. 157, p. 106159, 2021.
- [83] Y. Zheng, S. E. Li, J. Wang, D. Cao, and K. Li, “Stability and scalability of homogeneous vehicular platoon: Study on the influence of information flow topologies,” *IEEE Transactions on intelligent transportation systems*, vol. 17, no. 1, pp. 14–26, 2015.
- [84] V. Kolmanovskii and A. Myshkis, *Introduction to the Theory and Applications of Functional Differential Equations*. Dordrecht: Springer Netherlands, 1999.